Supplementary Information for:

TIPS-Pentacene Triplet Exciton Generation on PbS Quantum Dots Results from Indirect Sensitization

Christopher M. Papa[†], Sofia Garakyaraghi[†], Devin B. Granger[‡], John E. Anthony[‡], and Felix N. Castellano[†]*

[†]Department of Chemistry, North Carolina State University, Raleigh, North Carolina 27695-8204, United States.

[‡]Department of Chemistry, University of Kentucky, Lexington, Kentucky 40506-0055, United States.

*Corresponding author. E-mail: fncastel@ncsu.edu.

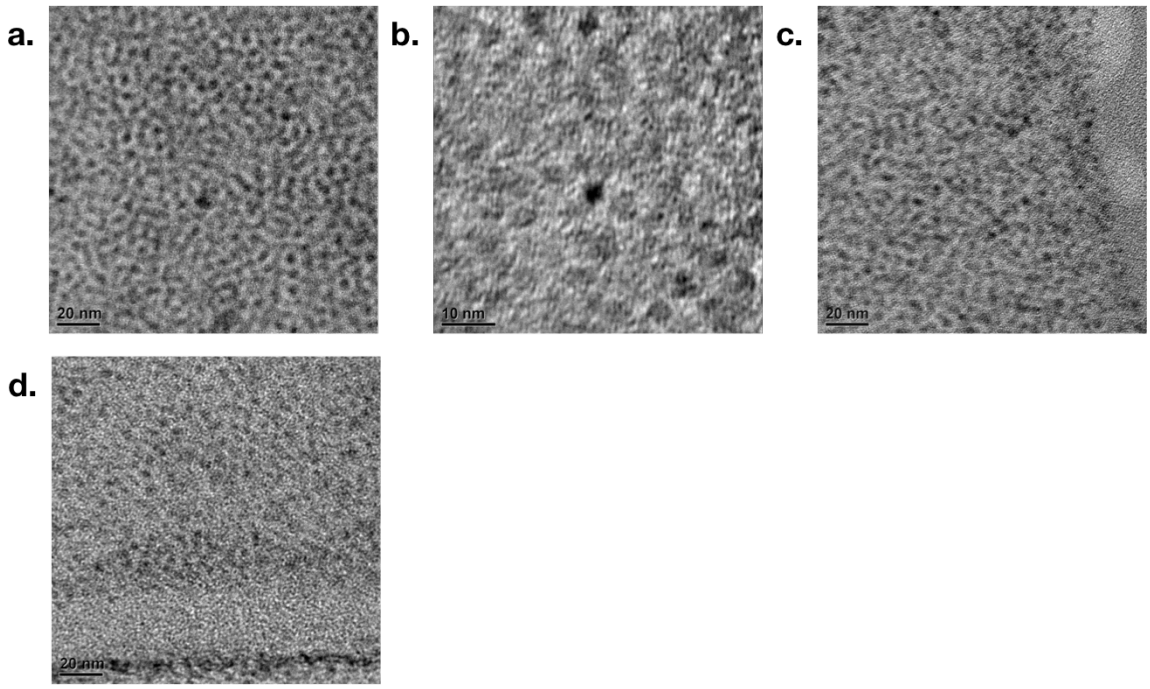

Figure S1. TEM images of PbS NCs with average diameters of **(a)** 3.3 nm, **(b)** 3.0 nm, **(c)** 2.9 nm, and **(d)** 2.2 nm.

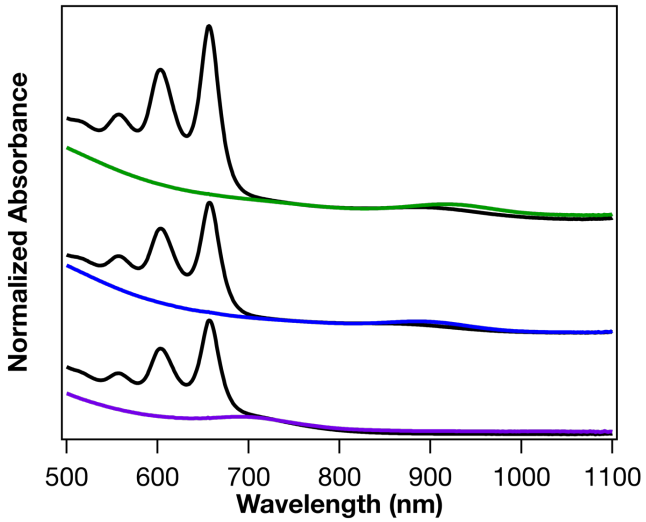

Figure S2. Electronic absorption spectra of PbS-1000 (red), PbS-970 (green), PbS-805 (purple) with their corresponding PbS-TPn hybrid materials (black lines, matching y-axis offset indicates matching NC size).

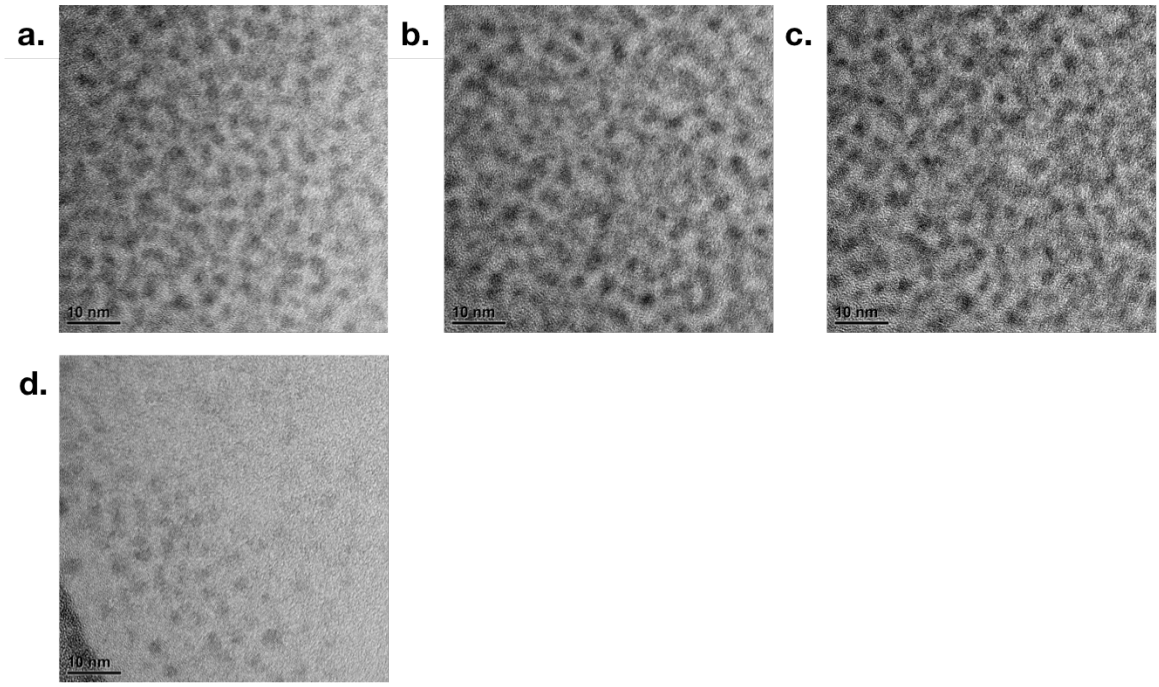

Figure S3. TEM images of **(a)** PbS-1075-TPn, **(b)** PbS-1000-TPn, **(c)** PbS-970-TPn, **(d)** PbS-805-TPn.

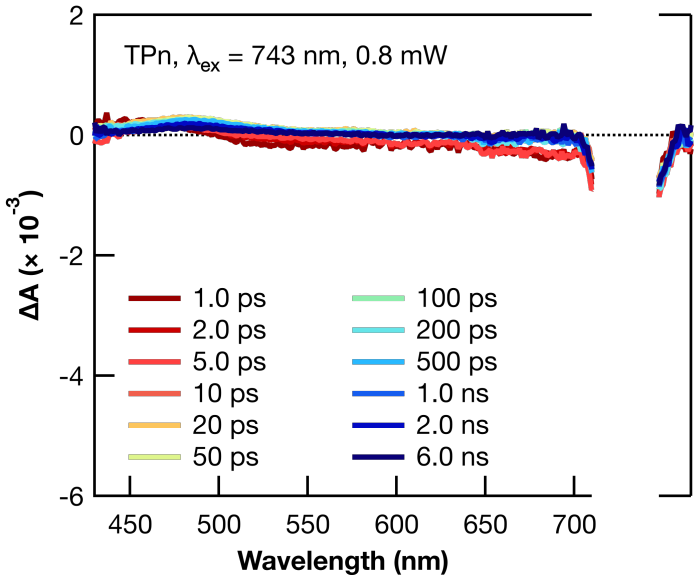

Figure S4. Ultrafast TA difference spectra of a solution of TPn in toluene following 743 nm pulsed laser excitation (0.80 μJ/pulse, 100 fs fwhm). The non-time-resolved spectral feature centered around 743 nm is scattered excitation.

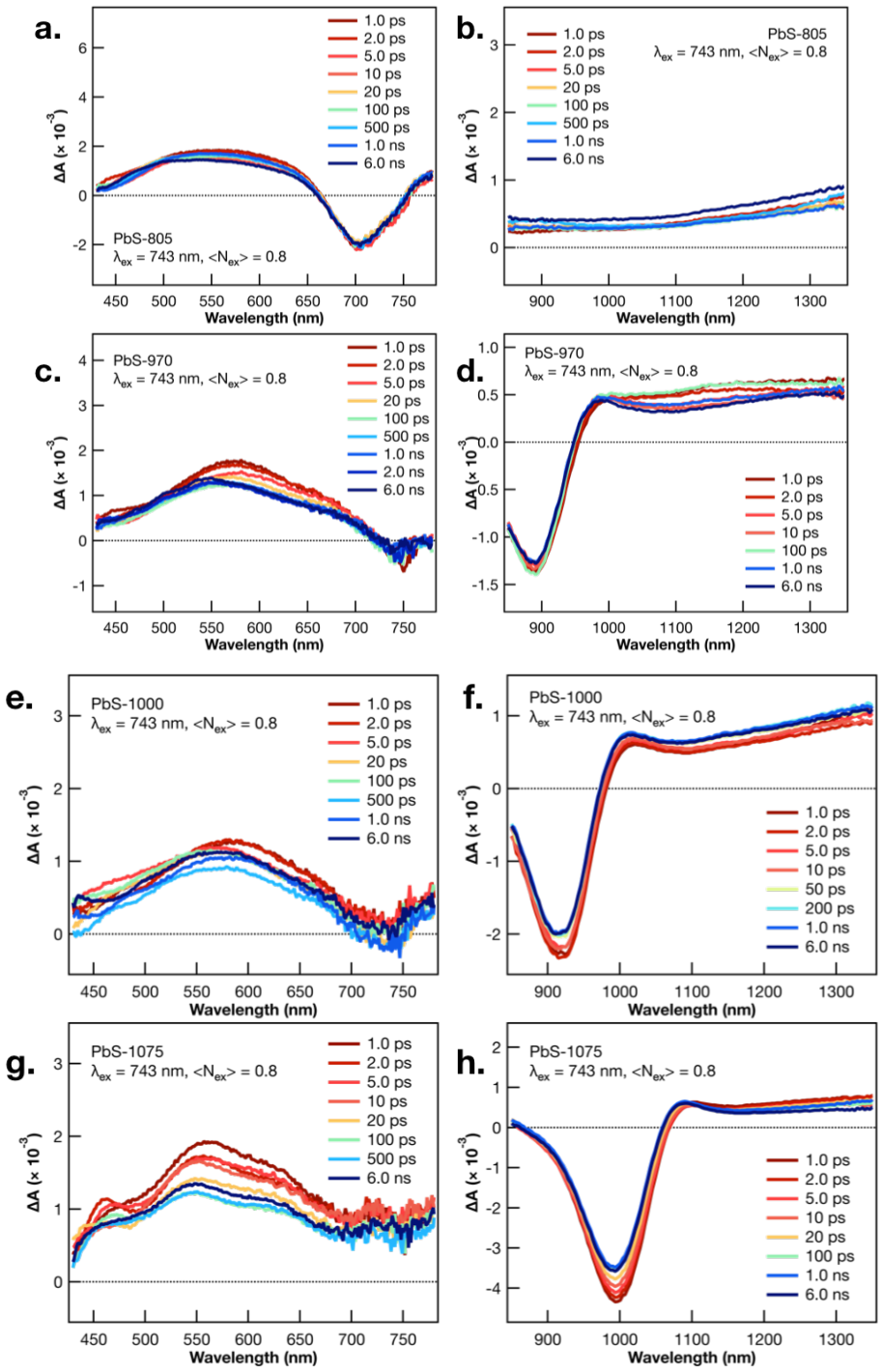

Figure S5. Ultrafast TA difference spectra of PbS nanocrystal suspensions in toluene following 743 nm pulsed laser excitation (0.15 μJ/pulse, 100 fs fwhm). The spectra correspond to PbS-805 in the **(a)** visible and **(b)** near-IR spectral regions, PbS-970 in the **(c)** visible and **(d)** NIR, PbS-1000 in the **(e)** visible and **(f)** NIR, and PbS-1075 in the **(g)** visible and **(h)** NIR. Time delays range from 1.0 ps (red) to 6.0 ns (blue).

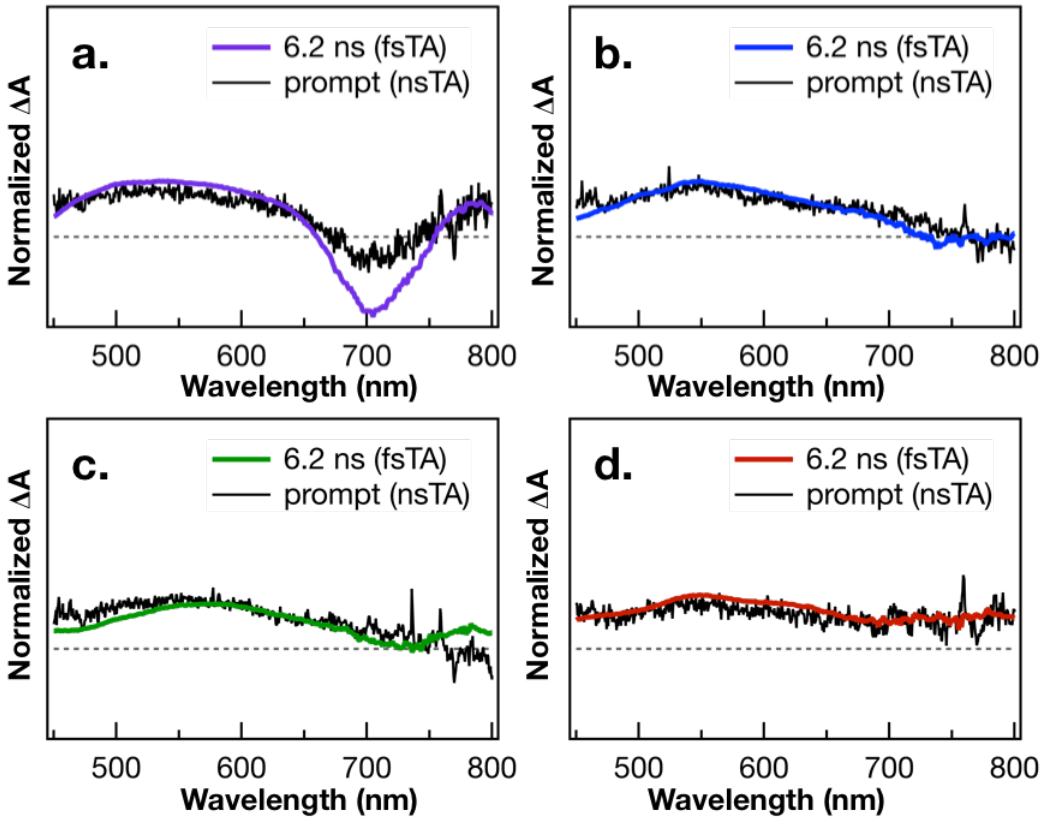

Figure S6. Comparison of normalized, ultrafast (0.15 μJ/pulse, 100 fs fwhm, 743 nm) TA difference spectra (colored) and normalized, nanosecond (1.0 mJ/pulse, 5 ns fwhm, 743 nm) TA difference spectra (black) of PbS nanocrystal suspensions in toluene following pulsed laser excitation. The spectra correspond to **(a)** PbS-805, **(b)** PbS-970, **(c)** PbS-1000, and **(d)** PbS-1075. Time delays are prompt for the nanosecond TA spectra and 6.2 ns for the ultrafast TA spectra.

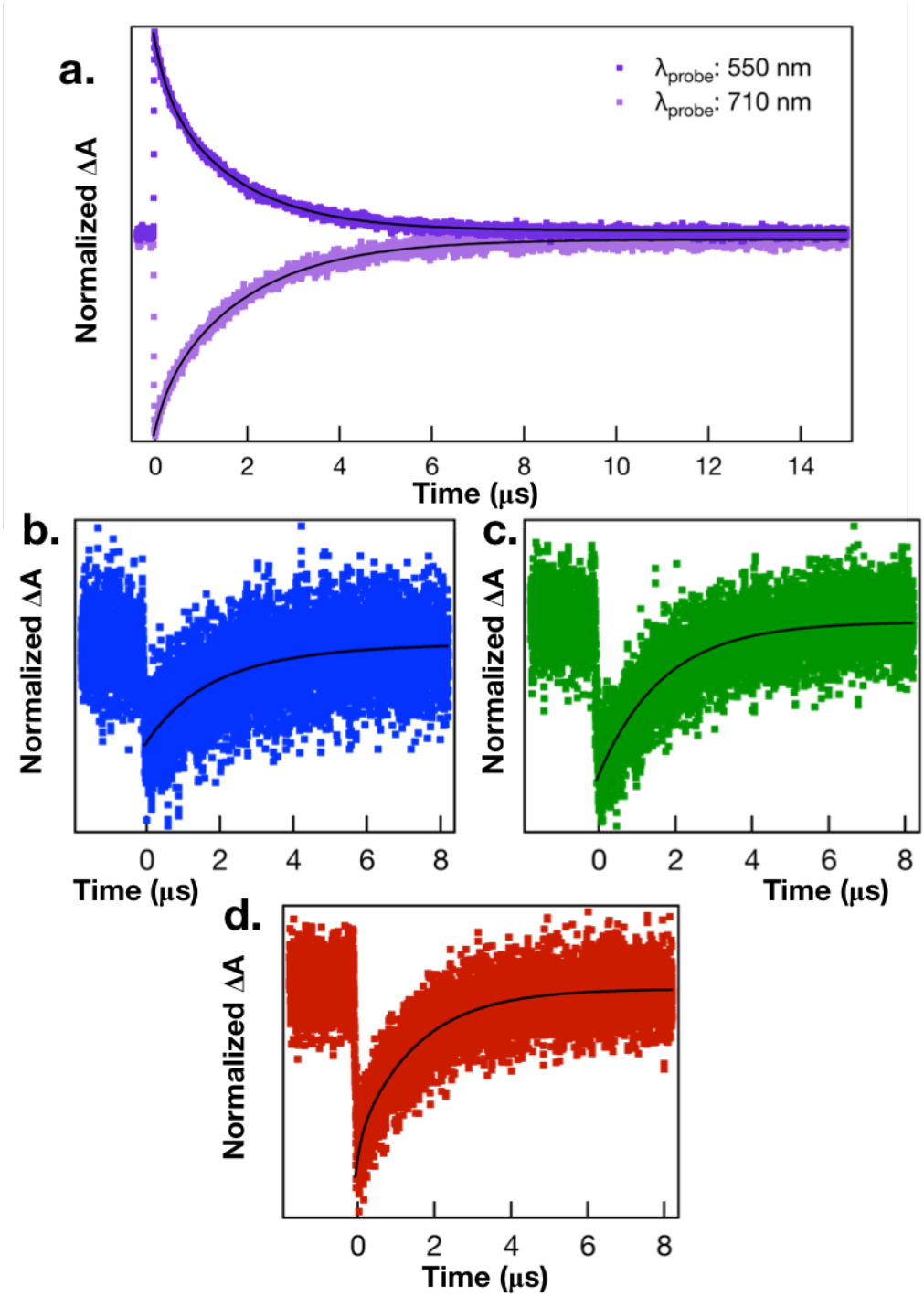

Figure S7. Nanosecond TA kinetics of **(a)** PbS-805, **(b)** PbS-970, **(c)** PbS-1000, and **(d)** PbS-1075 in toluene following pulsed excitation at 743 nm (1.0 mJ/pulse, 5 ns fwhm). The decays of the PbS NC induced absorption observed at 550 nm and the X1 bleaches at 710, 890, 920 and 1010 nm can be fit by biexponential functions (black lines) with time constants of 0.22 ± 0.07 and 1.8 ± 0.2 μs.

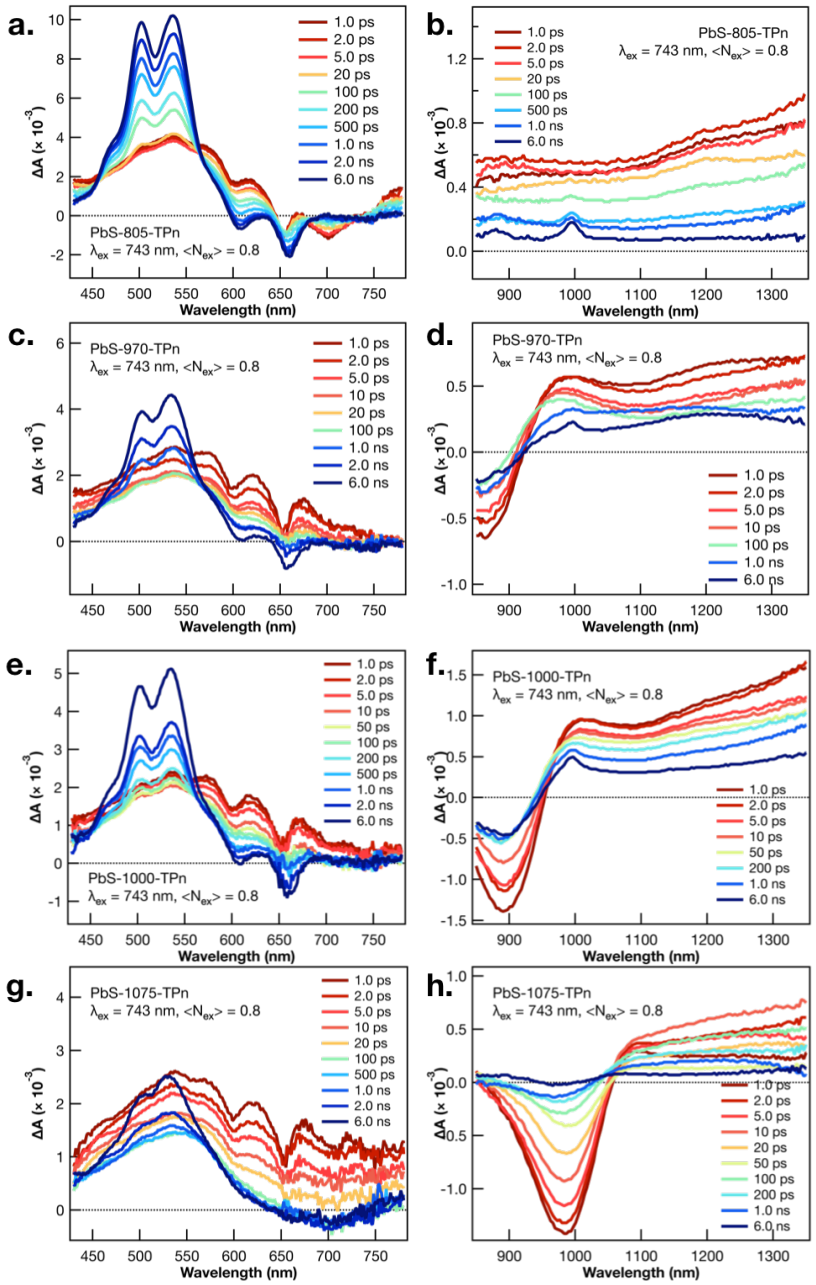

Figure S8. Ultrafast TA difference spectra of PbS-TPn nanocrystal-molecule hybrid materials suspended in toluene following 743 nm pulsed laser excitation (0.15 μJ/pulse, 100 fs fwhm). The spectra correspond to PbS-805-TPn in the **(a)** visible and **(b)** near-IR spectral regions, PbS-970-TPn in the **(c)** visible and **(d)** NIR, PbS-1000-TPn in the **(e)** visible and **(f)** NIR, and PbS-1075-TPn in the **(g)** visible and **(h)** NIR. Time delays range from 1.0 ps (red) to 6.0 ns (blue).

	τ_1 (ps) 528-540 nm & GSB	GSB λ_{probe} (nm)	τ_2 (ns) 528-540 nm
PbS-805-TPn	1.7 – 2.4	698 – 710	0.35 – 0.41
PbS-970-TPn	5.4 – 10.5	851 – 863	2.7
PbS-1000-TPn	5.7 – 7.3	888 – 900	2.5
PbS-1075-TPn	16 – 27	981 – 993	9.4

Table S1. Decay constants obtained from fitting kinetic traces at single wavelengths of TA data for PbS-TPn nanocrystal-molecule hybrid materials suspended in toluene following pulsed excitation at 743 nm (0.15 μJ/pulse, 100 fs fwhm). Values for the first time constant were determined by fitting the attenuation of the PbS NC features from 528 – 540 nm (photoinduced absorption) and the ground state bleach (GSB column), while values for the second time constant were determined from monitoring the rise of the characteristic ^{3}TPn signal from 528 – 540 nm.

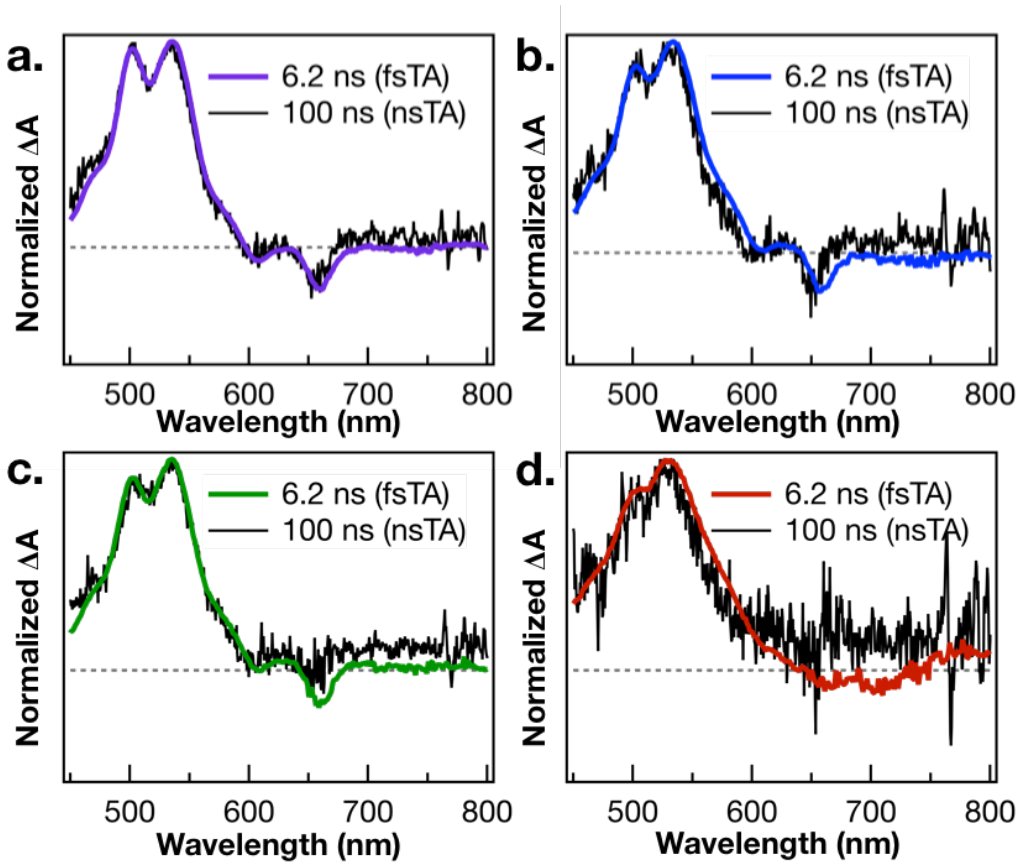

Figure S9. Comparison of normalized, ultrafast (0.15 μJ/pulse, 100 fs fwhm, 743 nm) TA difference spectra (colored) and normalized, nanosecond (1.0 mJ/pulse, 5 ns fwhm, 743 nm) TA difference spectra (black) of PbS-TPn hybrid material suspensions in toluene following pulsed laser excitation. The spectra correspond to **(a)** PbS-805-TPn, **(b)** PbS-970-TPn, **(c)** PbS-1000-TPn, and **(d)** PbS-1075-TPn. Time delays are 6.2 ns for the ultrafast TA spectra and 100 ns for the nanosecond TA spectra.

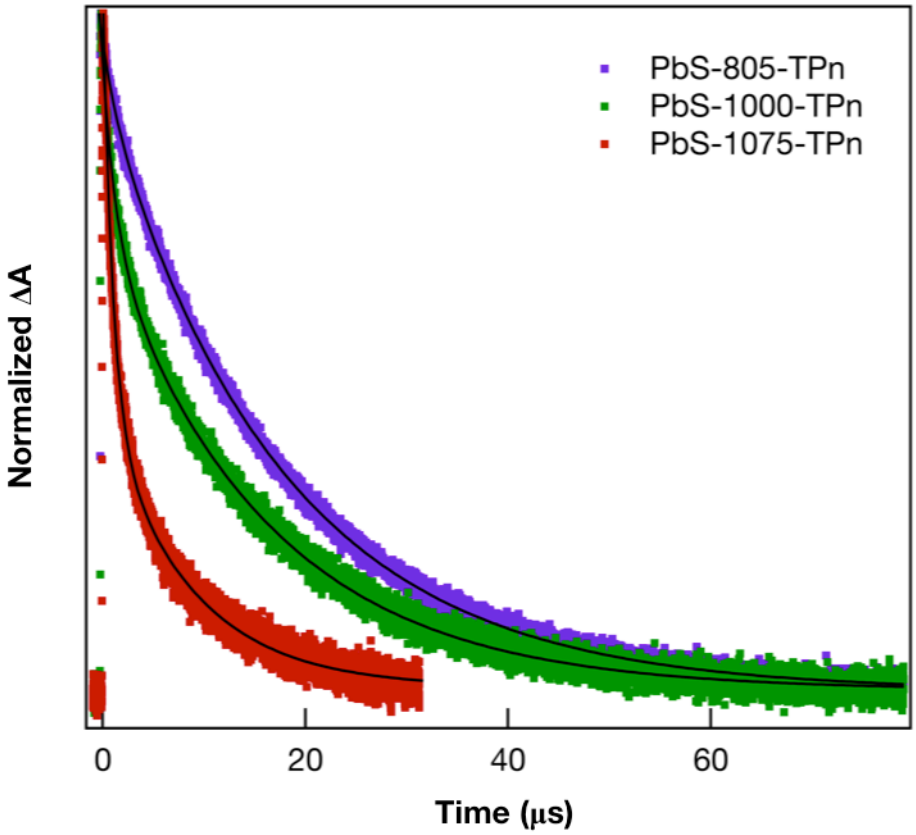

Figure S10. Nanosecond TA kinetics of PbS-TPn nanocrystal-molecule hybrid materials suspended in toluene following pulsed excitation at 743 nm (1.0 mJ/pulse, 5 ns fwhm). The decays of the ^{3}TPn feature observed at 534 nm are fit by biexponential functions (black lines) with time constants given in Table S2. PbS-970-TPn TA kinetics omitted for clarity.

	τ_1 (μs)	τ_2 (μs)
PbS-805-TPn	11.7 ± 0.2	22.3 ± 0.9
PbS-970-TPn	1.34 ± 0.09	15.1 ± 0.2
PbS-1000-TPn	1.40 ± 0.02	15.6 ± 0.1
PbS-1075-TPn	0.87 ± 0.06	6.85 ± 0.06

Table S2. Decay constants obtained from fitting kinetic traces (λ_{probe} = 534 nm) displayed in Fig. S9 to biexponential functions. Data is from TA kinetics of PbS-TPn nanocrystal-molecule hybrid materials suspended in toluene following pulsed excitation at 743 nm (1.0 mJ/pulse, 5 ns fwhm).

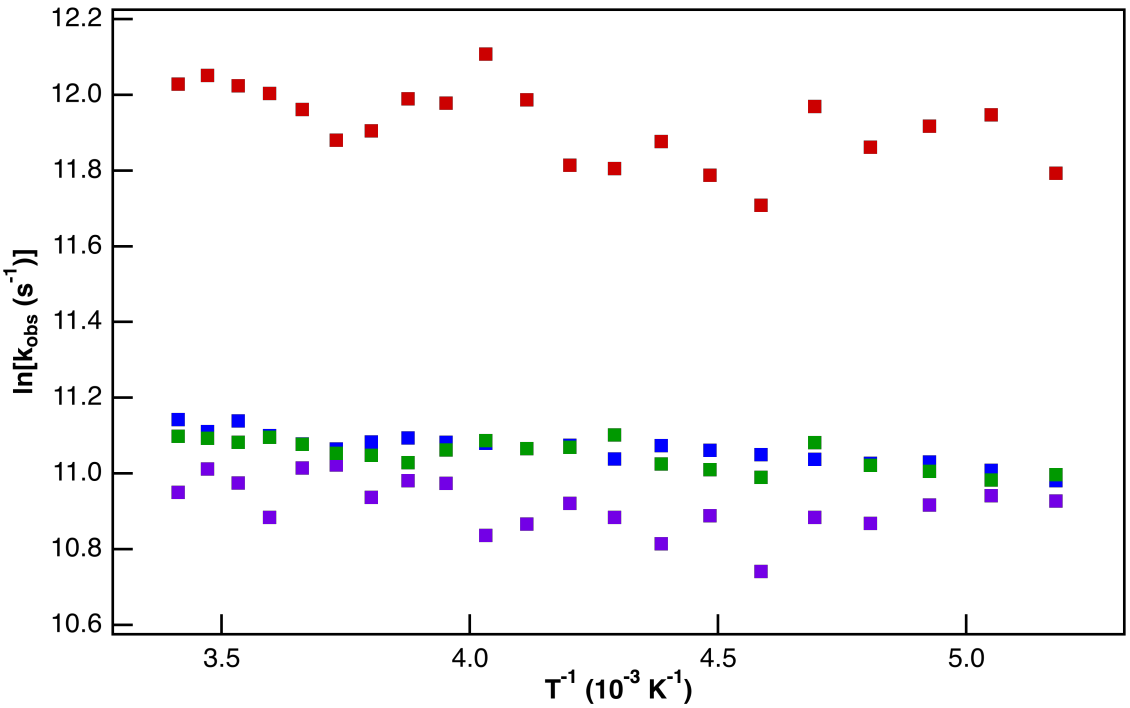

Figure S11. Rate constants from temperature-dependent nanosecond TA kinetics of PbS-TPn nanocrystal-molecule hybrid materials suspended in toluene following pulsed excitation at 743 nm (1.0 mJ/pulse, 5 ns fwhm). The logarithm of the rate constants determined by mathematical fitting of the ^{3}TPn decay observed at 534 nm is compared to the inverse of the temperature at which the decay was recorded.

	τ_1 (ps)	k_1 ($\times 10^9$ s^{-1})	τ_2 (ns)	k_2 ($\times 10^6$ s^{-1})	τ_3
PbS-805-TPn	3 ± 1	18 ± 6	0.39 ± 0.07	140 ± 40	infinite
PbS-970-TPn	4.0 ± 0.1	8 ± 2	1.8 ± 0.3	20 ± 8	infinite
PbS-1000-TPn	6.8 ± 0.3	4 ± 2	1.1 ± 0.4	30 ± 20	infinite
PbS-1075-TPn	12.3 ± 0.2	1.6 ± 0.5	5 ± 2	5 ± 3	infinite

Table S3. Raw time constants and per-TPn-adjusted rate constants obtained by modeling ultrafast TA spectra for PbS-TPn materials. Corresponding basis spectra are displayed in Figure 3 of the main text. The third time constant is "infinite" over the 6.2 ns delay stage of the ultrafast TA experiment. For accurate lifetimes for the relaxation of ^{3}TPn, see Table S2.

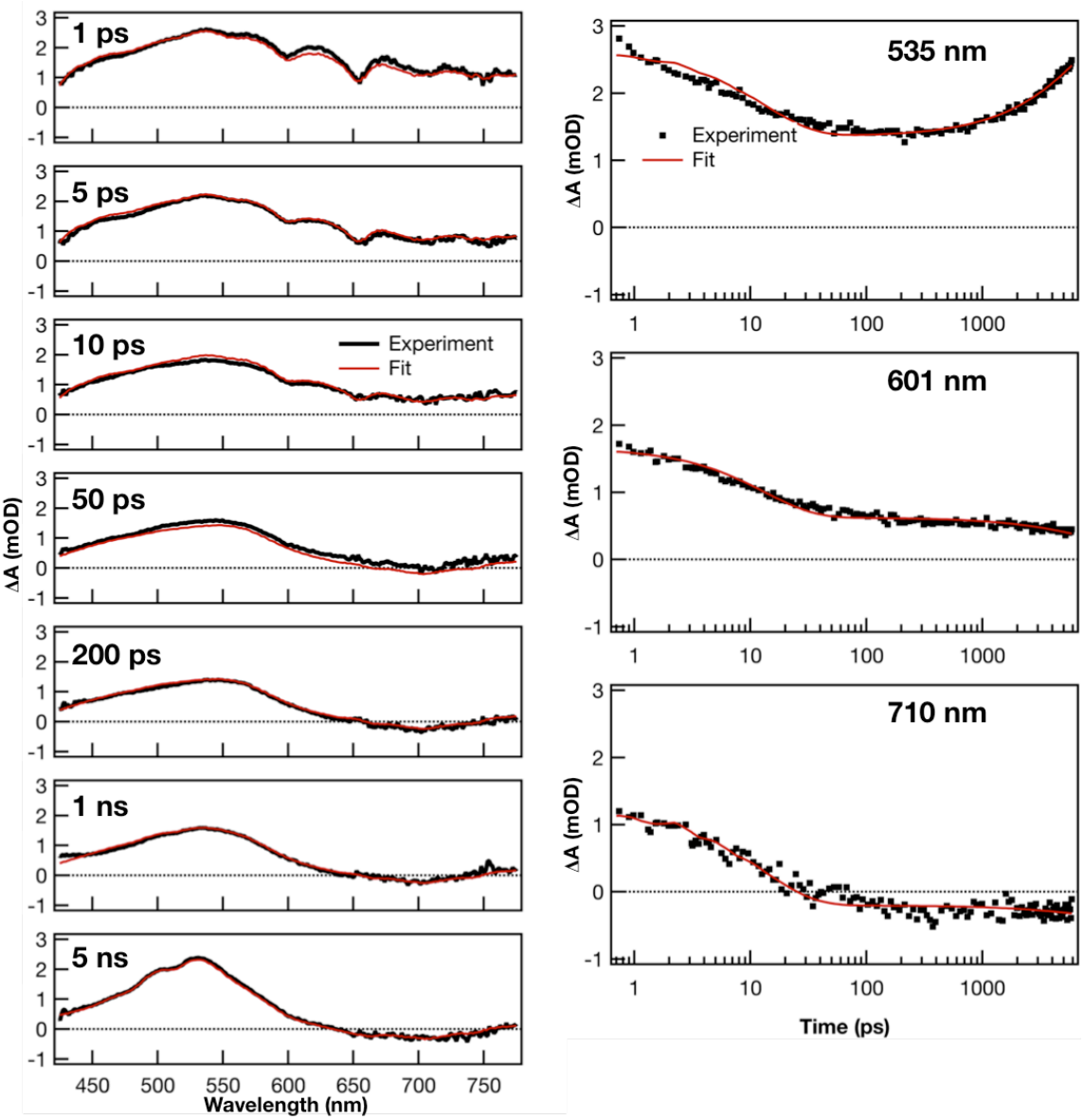

Figure S12. Experimental PbS-1075-TPn ultrafast TA spectra (black) probed in the visible region of the electromagnetic spectrum compared to the fit modeled by linear decomposition (red). Three DADS were necessary to reproduce the changes in the spectra. Time constants for first-order interconversion between the DADS were found to be 13.2 ps and 8.1 ns as described in the main text.

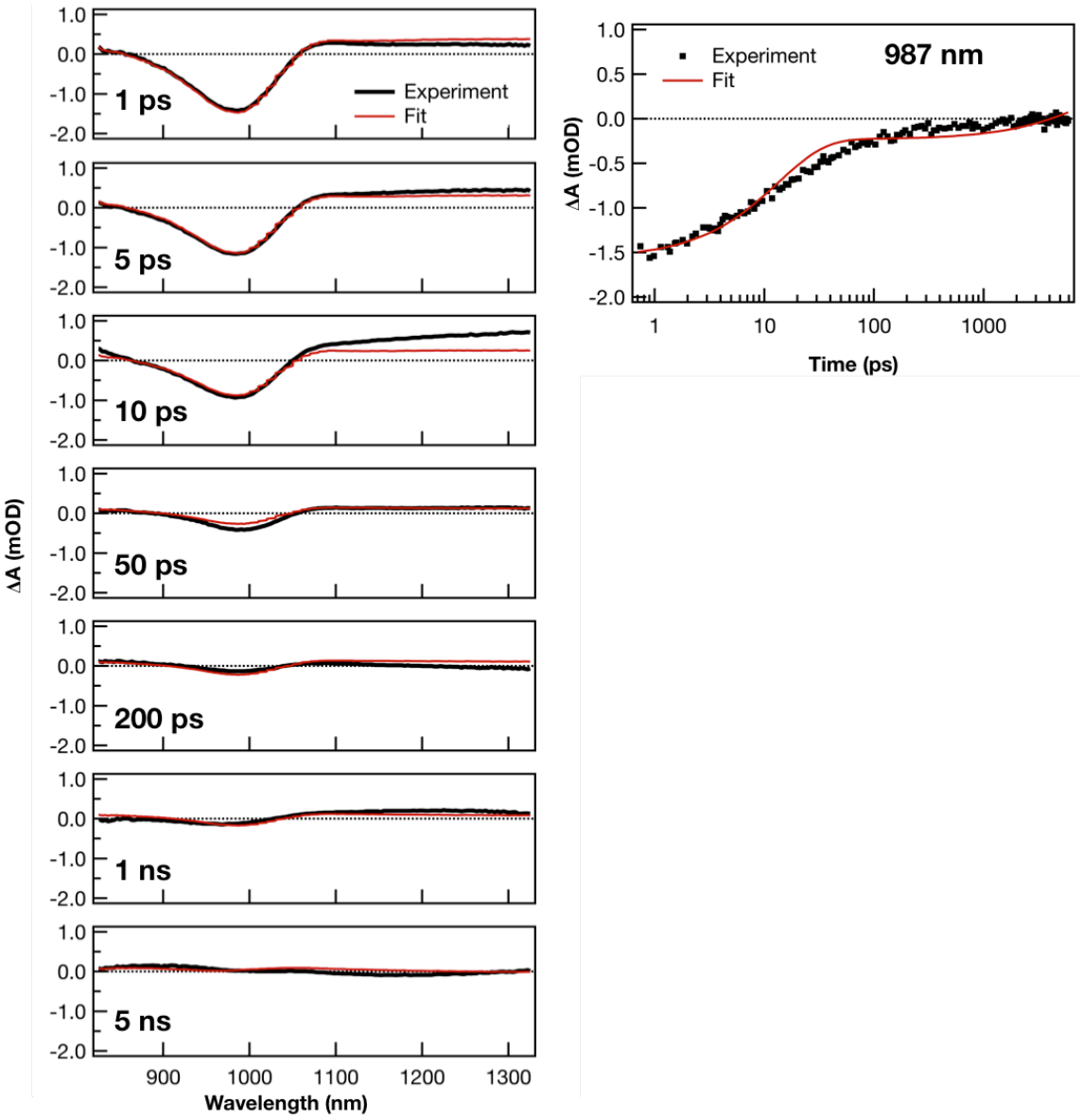

Figure S13. Experimental PbS-1075-TPn ultrafast TA spectra (black) probed in the near-infrared region of the electromagnetic spectrum compared to the fit modeled by linear decomposition (red). Three DADS were necessary to reproduce the changes in the spectra. Time constants for first-order interconversion between the DADS were found to be 13.2 ps and 8.1 ns as described in the main text.

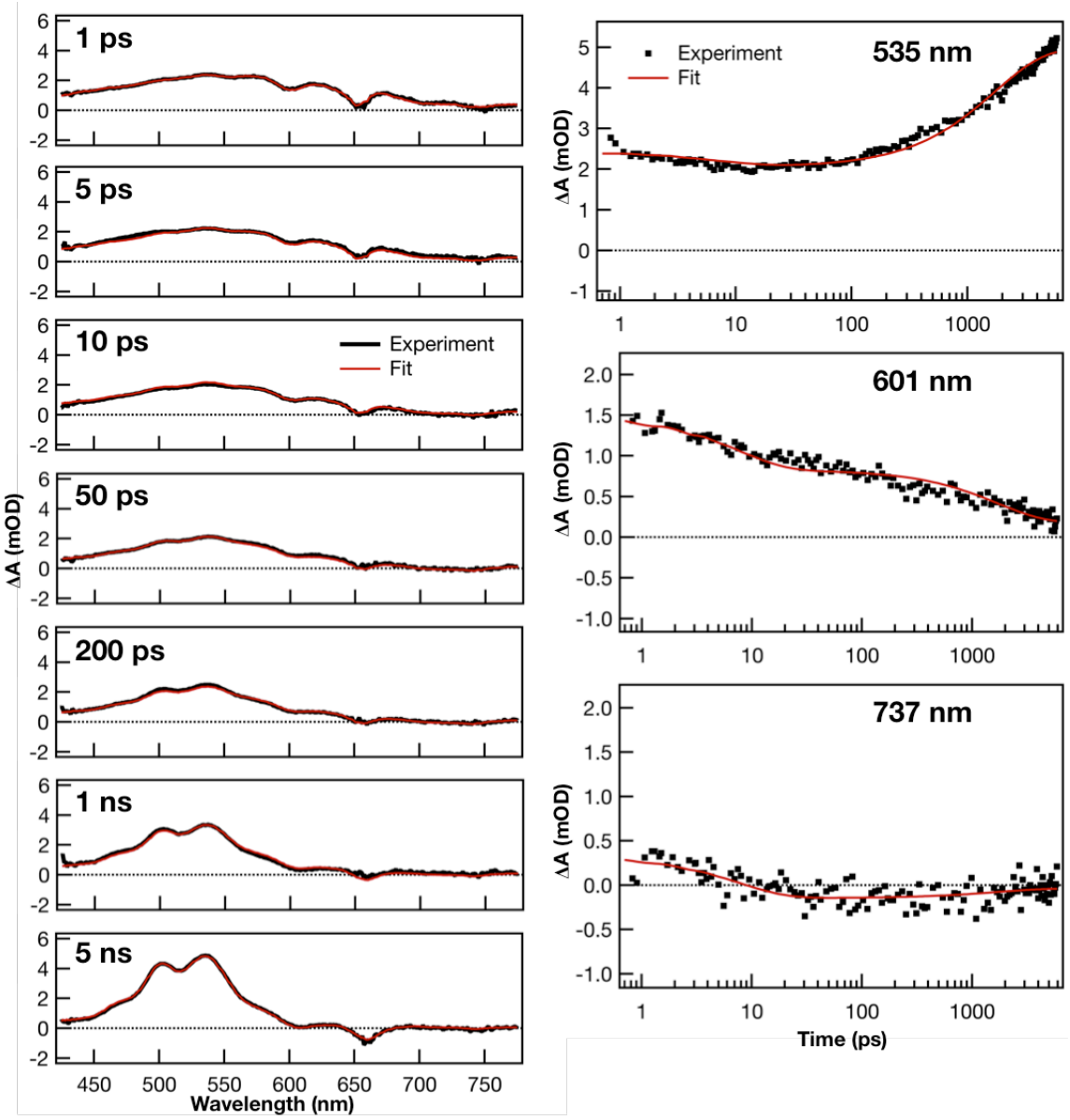

Figure S14. Experimental PbS-1000-TPn ultrafast TA spectra (black) probed in the visible region of the electromagnetic spectrum compared to the fit modeled by linear decomposition (red). Three DADS were necessary to reproduce the changes in the spectra. Time constants for first-order interconversion between the DADS were found to be 7.6 ps and 1.7 ns as described in the main text.

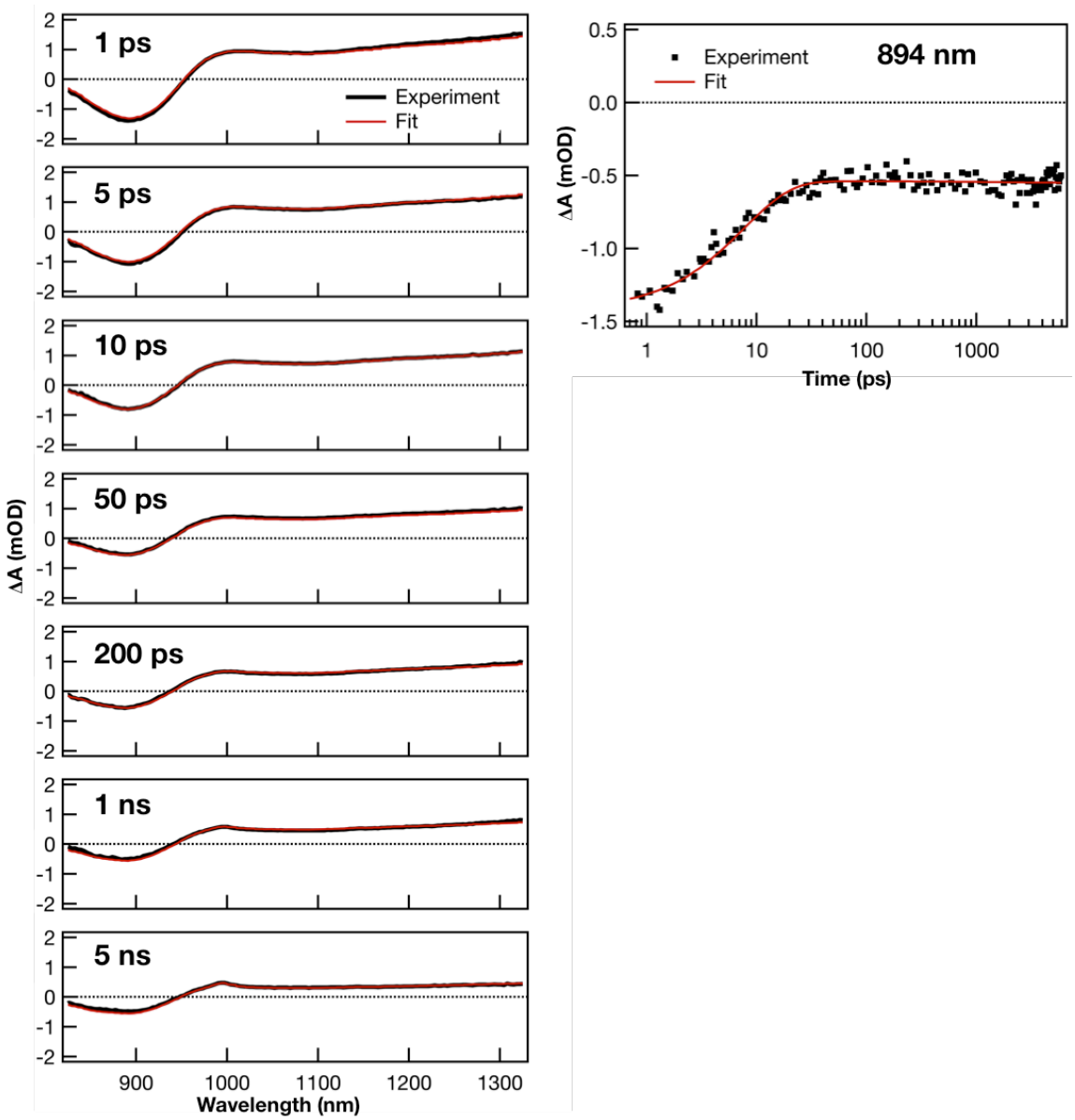

Figure S15. Experimental PbS-1000-TPn ultrafast TA spectra (black) probed in the near-infrared region of the electromagnetic spectrum compared to the fit modeled by linear decomposition (red). Three DADS were necessary to reproduce the changes in the spectra. Time constants for first-order interconversion between the DADS were found to be 7.6 ps and 1.7 ns as described in the main text.

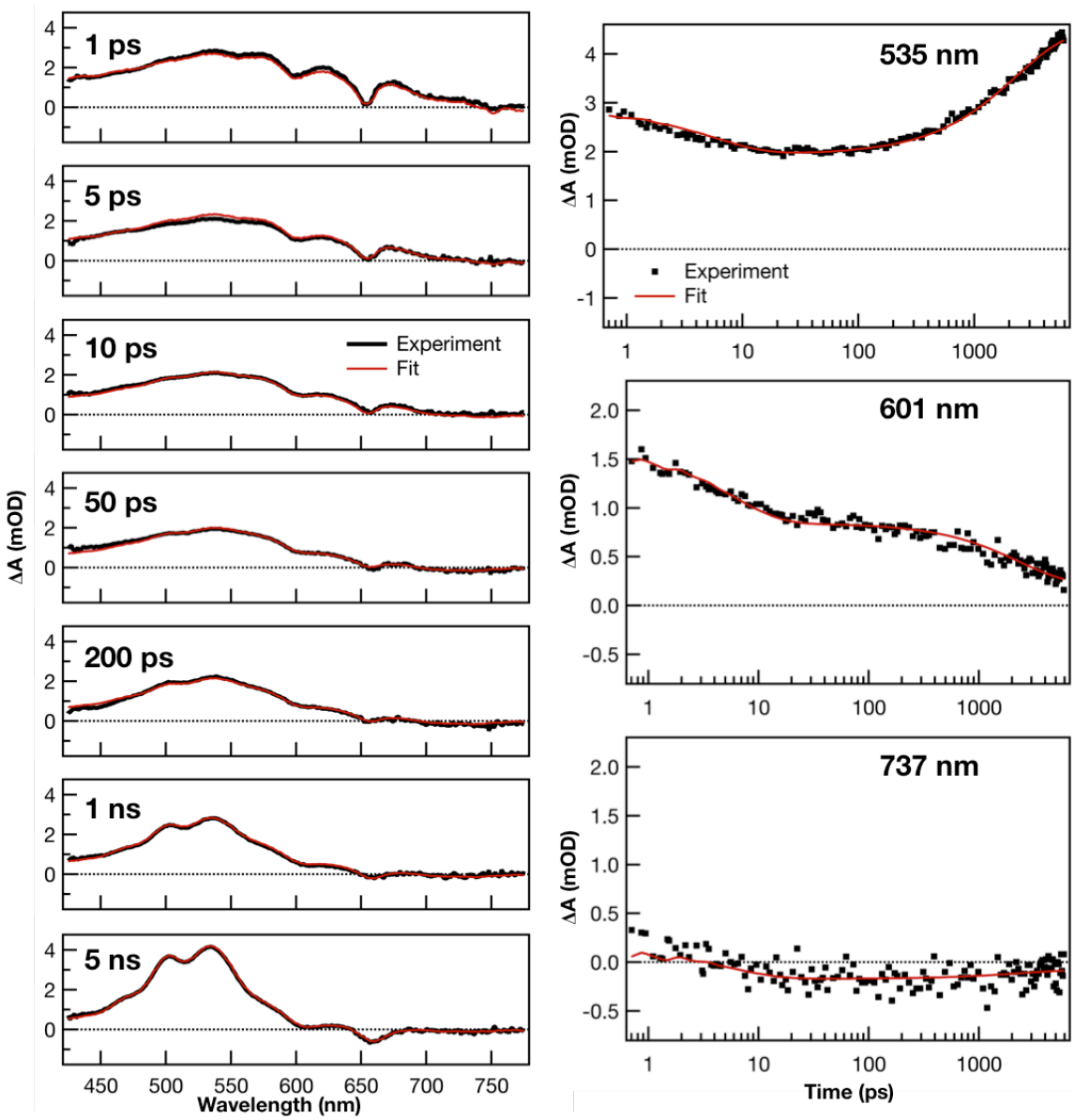

Figure S16. Experimental PbS-970-TPn ultrafast TA spectra (black) probed in the visible region of the electromagnetic spectrum compared to the fit modeled by linear decomposition (red). Three DADS were necessary to reproduce the changes in the spectra. Time constants for first-order interconversion between the DADS were found to be 6.0 ps and 2.3 ns as described in the main text.

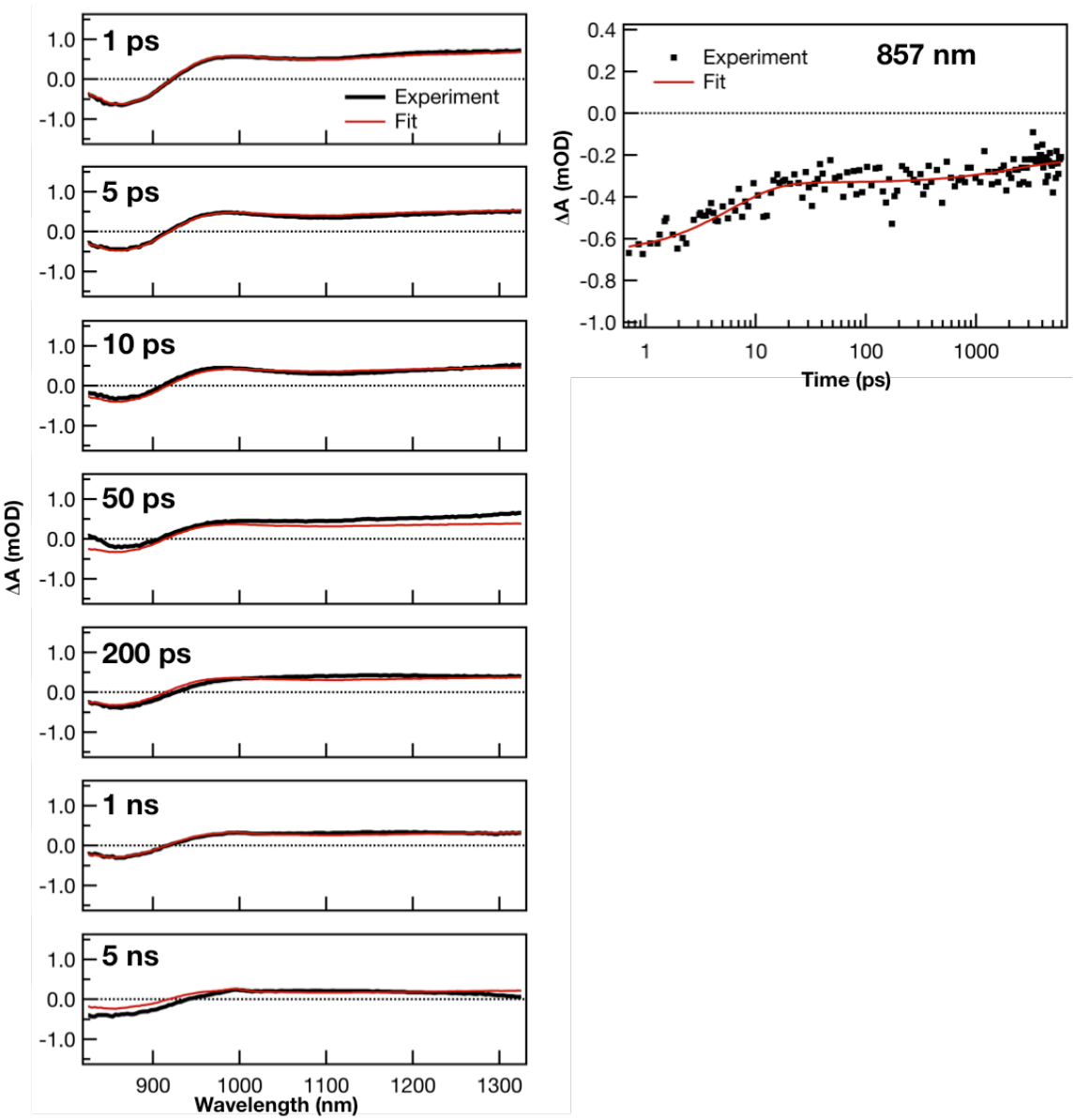

Figure S17. Experimental PbS-970-TPn ultrafast TA spectra (black) probed in the near-infrared region of the electromagnetic spectrum compared to the fit modeled by linear decomposition (red). Three DADS were necessary to reproduce the changes in the spectra. Time constants for first-order interconversion between the DADS were found to be 6.0 ps and 2.3 ns as described in the main text.

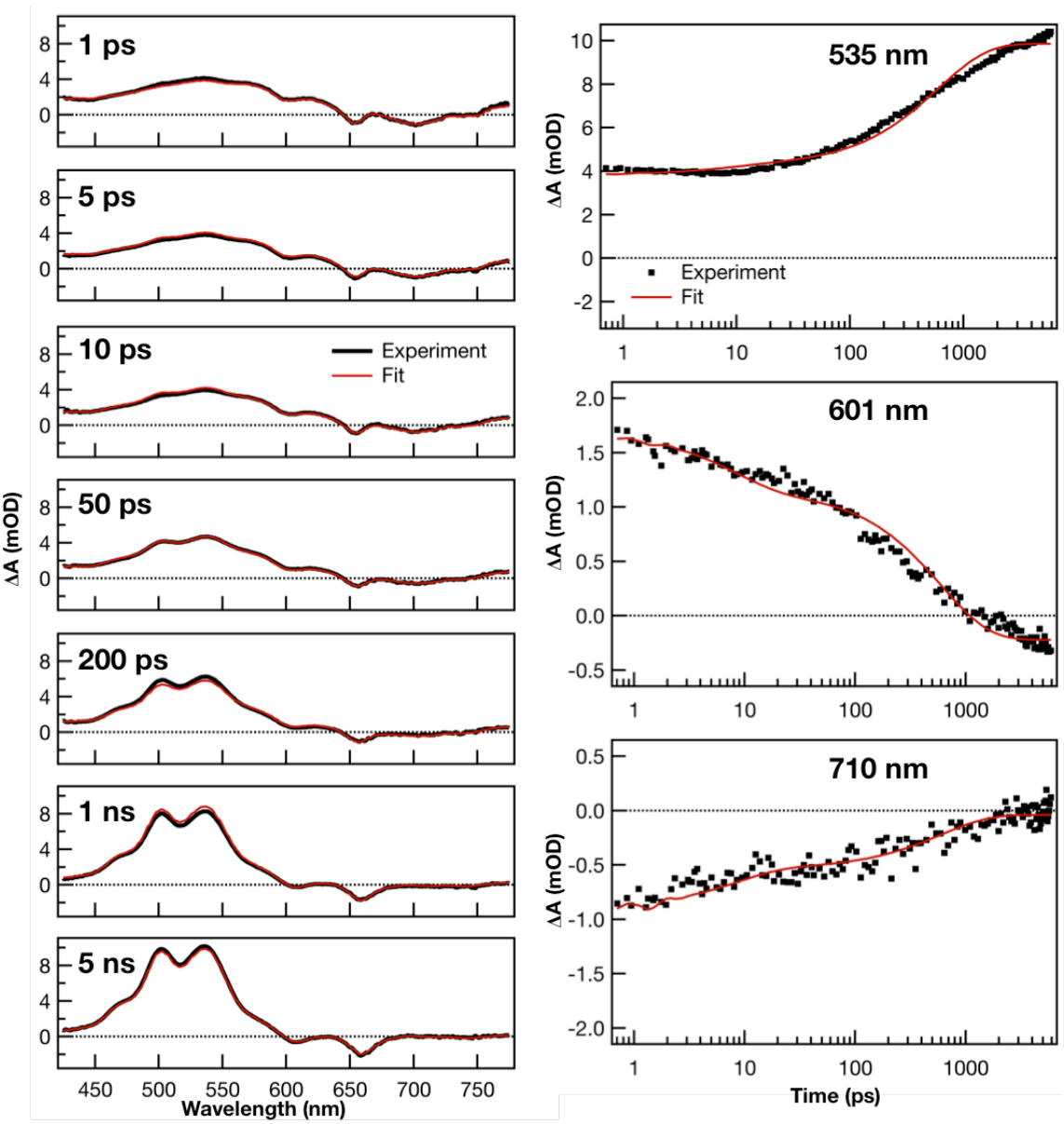

Figure S18. Experimental PbS-805-TPn ultrafast TA spectra (black) probed in the visible region of the electromagnetic spectrum compared to the fit modeled by linear decomposition (red). Three DADS were necessary to reproduce the changes in the spectra. Time constants for first-order interconversion between the DADS were found to be 7.9 ps and 0.60 ns as described in the main text. This sample was absorbance matched at excitation to the PbS-TPn materials.

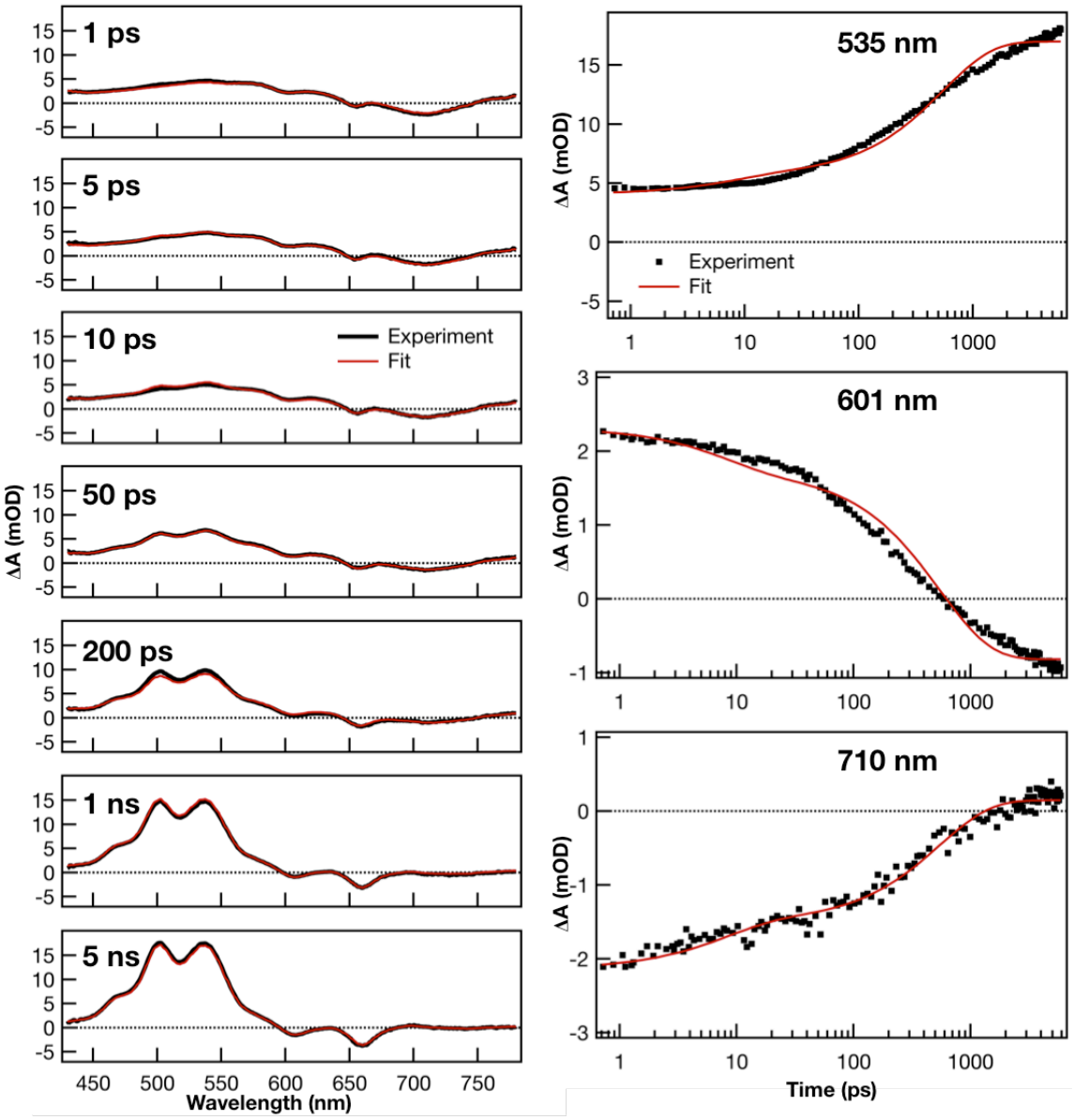

Figure S19. Experimental PbS-805-TPn ultrafast TA spectra (black) probed in the visible region of the electromagnetic spectrum compared to the fit modeled by linear decomposition (red). Three DADS were necessary to reproduce the changes in the spectra. Time constants for first-order interconversion between the DADS were found to be 7.9 ps and 0.55 ns as described in the main text. This sample was absorbance matched at excitation to the PbS-CdS-TPn materials.